NATIONAL AERONAUTICS AND SPACE ADMINISTRATION

Technical Report 32-1451

Hypersonic Blunt-Body Flow of a Radiating Gas at Low Density

W. A. Schneider

JET PROPULSION LABORATORY

CALIFORNIA INSTITUTE OF TECHNOLOGY

PASADENA, CALIFORNIA

July 1, 1970

NATIONAL AERONAUTICS AND SPACE ADMINISTRATION

Technical Report 32-1451

Hypersonic Blunt-Body Flow of a Radiating Gas at Low Density

W. A. Schneider

JET PROPULSION LABORATORY
CALIFORNIA INSTITUTE OF TECHNOLOGY
PASADENA, CALIFORNIA

July 1, 1970

Prepared Under Contract No. NAS 7-100
National Aeronautics and Space Administration

Preface

The work described in this report was performed by the Environmental Sciences Division of the Jet Propulsion Laboratory.

Acknowledgment

This report presents results of research accomplished at the Jet Propulsion Laboratory while the author was pursuing a Senior Postdoctoral Research Associateship administered by the National Research Council and supported by the National Aeronautics and Space Administration.

Contents

Figures

Contents (contd)

Figures (contd)

Abstract

The effect of radiation on hypersonic viscous flow at low densities is studied. Cheng's two-layer flow model (dividing the flow field into a thin shock layer and a thin shock transition zone) is used to simplify the Navier–Stokes equations. Radiation is taken into account by adding an emission term to the energy equation. Because of the low density, self-absorption may be neglected but nonequilibrium effects become important. Estimates show that vibration, dissociation, and ionization can be assumed to be frozen in the density–velocity regime of interest, but the process of electron excitation has to be investigated on the basis of finite relaxation times. Rate equations for emission due to nonequilibrium radiation from various band systems are derived, and the effect of "collision limiting" is discussed in the light of these equations. The rate constants for the most important molecular band systems in air are determined experimentally. Finally, numerical results for the flow field in the stagnation region and for the heat transfer coefficient are discussed.

Hypersonic Blunt-Body Flow of a Radiating Gas at Low Density

I. Introduction

In the past 10 years, there has been much interest in low-density[1] hypersonic flow in theoretical and experimental research. Some of the problems in low-density hypersonic flow are shown in Fig. 1 which depicts various flow regimes depending on free-stream velocity and altitude or free-stream density. At sufficiently high densities of gas, the well-known boundary layer concept is valid. This concept proposes that there is an inviscid shock layer where viscosity and heat conduction can be neglected, and a thin boundary layer where viscosity and heat conduction are important. When the density decreases, the Reynolds number also decreases and the boundary layer and shock wave become thicker. At sufficiently low densities, the shock wave and the viscous shock layer combine to form a so-called merged layer. Any further decrease in density is not in the domain of continuum flow. Figure 1 shows several different regimes as originally defined by Probstein (Ref. 1) and Hayes and Probstein (Ref. 2). Other authors have defined somewhat different regimes (Refs. 3 and 4). In the analysis to be presented in this paper, the definitions used by Probstein are utilized, but only for reference purposes.

So far only viscosity and heat conduction have been mentioned, but at high free-stream velocities, radiation effects in the hot gas cap surrounding a blunt body may also be important. Generally, radiation effects become less important as gas density decreases. Therefore, it is not clear at first whether or not radiation is of importance at the low densities with which we are concerned. In fact, Teare et al., (Ref. 5) have concluded from estimates made about eight years ago that heat transfer due to radiation is rather negligible when compared with convective heat transfer in the merged layer regime. However, these earlier estimates *under*estimate the radiative heat transfer and *over*estimate the convective heat transfer in the merged layer regime for several reasons discussed in Section VIII.

Thus, the question of the importance of radiative heating in hypersonic low-density flow was still open, and

[1]The term "low density" used in this report is defined to be a density low enough to make the boundary layer concept *not* acceptable, but high enough to justify a continuum approach. In other words, we direct our attention to the regime covered by the viscous and the merged layers.

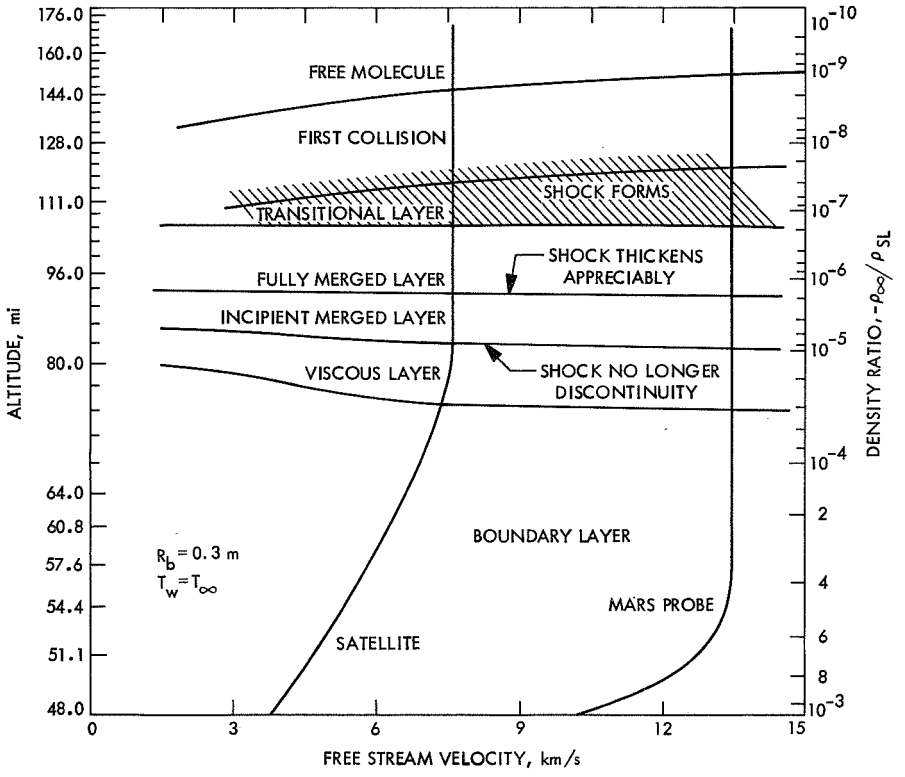

Fig. 1. Rarefied gas flow regimes for the stagnation region of a highly cooled blunt body (after Probstein)

was a prime reason, as was the study of nonequilibrium radiation effects in a realistic case where molecular and radiative transport processes are strongly coupled, for undertaking this study. The results of this investigation show that radiation effects can play an important role in the merged layer regime, even at moderate speeds around the parabolic speed ($\approx$11 km/s).

II. Flow Model

As a consequence of the large number of investigators of low-density (low Reynolds number) hypersonic flow, there is quite a number of methods to describe such a flow (Refs. 2, 3, and 6). However, to be useful in the problem of interest, the method should have certain special properties:

(1) It must be possible to generalize the method so that it is applicable to a general fluid including radiation and nonequilibrium effects.

(2) The method must be simple enough to make numerical solutions of this generalized problem tractable with present computers.

(3) It should be applicable not only in the stagnation region, but in the whole field from the stagnation region to the locally supersonic region.

The approach that satisfies these conditions best is (at least to the author's knowledge) the two-layer model developed by Cheng (Refs. 7 and 8). Although the results shown in the present paper are restricted to the stagnation region, the method can also be used outside the stagnation region; however, the numerical solution would be rather time-consuming. Assume a blunt body with nose radius R_b in a hypersonic low-density free stream (Fig. 2), and neglect radiation for the moment. The disturbed flow field is divided into two layers: (1) the "shock layer" where the pressure is very high and approximately equal to the Rankine–Hugoniot pressure behind an ordinary (adiabatic) shock wave, and (2) the "transition zone" (or "shock structure") defined as the zone through which transition from the low free-stream pressure to the high Rankine–Hugoniot pressure is completed by molecular collisions. Both layers are assumed to be thin in comparison with the nose radius of the body. This assumption, although stated *a priori*, may be justified later by results that show that shock-layer thickness

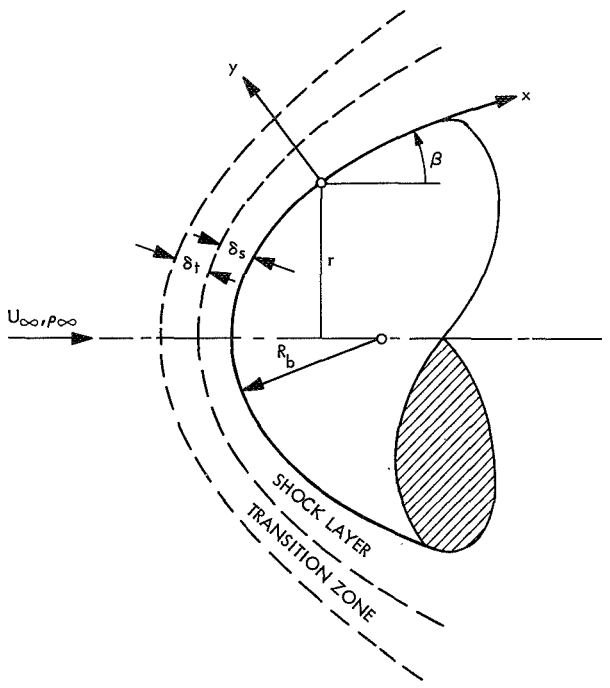

Fig. 2. Two-layer flow model and coordinate system

over body radius is of the order of the density ratio across the "shock" [$\sim(\gamma-1)/(\gamma+1)$ for a perfect gas], and that transition zone thickness over body radius is of the order of Re_s^{-1}, where $Re_s = \rho_\infty U_\infty R_b/\mu_s$ is the shock-layer Reynolds number with μ_s as a characteristic value of viscosity in the shock layer (Refs. 6 and 9). That Re_s^{-1} is much less than 1 is a necessary condition for continuum flow (Appendix A) so this condition is not a new restriction of the applicability of the theory. The boundary between the two layers is called the "shock interface" and is itself a layer of finite, but negligible, thickness.

By application of the thin-layer assumption, conservation equations for a viscous and heat-conducting fluid can be simplified substantially. It is advantageous to use a boundary-layer type coordinate system x,y (Fig. 2) and to satisfy the continuity equation identically by introducing a stream function ψ that represents mass flow per unit depth for two-dimensional flows, and mass flow per unit azimuthal angle (in radians) for axisymmetric flows. Upon reduction of the problem to the flow in the vicinity of the axis of symmetry (the "stagnation region") of an axisymmetric body, Eqs. (1) and (2) are obtained for the shock layer (see Ref. 7 or Appendix B). Equation (1) is the x-momentum equation (with the pressure-gradient term eliminated by the y-momentum equation):

$$\bar{u}^2 - \zeta\bar{u}\frac{d\bar{u}}{d\zeta} - \frac{1}{\epsilon_0 Re_0}\frac{\bar{u}}{\zeta}\frac{d}{d\zeta}\left(N\frac{\bar{u}}{\zeta}\frac{d\bar{u}}{d\zeta}\right) = 2\epsilon\bar{H}\left(1+\int_\zeta^1 \bar{u}\zeta\, d\zeta\right) \tag{1}$$

and Eq. (2) is the energy equation:

$$\bar{u}\zeta\frac{d\bar{H}}{d\zeta} + \frac{1}{\epsilon_0 Re_0}\frac{\bar{u}}{\zeta}\frac{d}{d\zeta}\left(\frac{N}{Pr}\frac{\bar{u}}{\zeta}\frac{d\bar{H}}{d\zeta}\right) = 0 \tag{2}$$

The y-momentum equation simply states that the pressure remains constant along the axis of symmetry in the present approximation. The quantity $\bar{u}$ is the dimensionless velocity component in x-direction (see Fig. 2),

$$\bar{u} = \frac{u}{U_\infty \cos\beta} \tag{3}$$

$\bar{H}$ is the dimensionless total enthalpy, which, for a stagnation region in hypersonic flow, can be written as:

$$\bar{H} = \frac{H}{H_\infty} = \frac{2h}{U_\infty^2} + \cdots \tag{4}$$

and ζ is a dimensionless variable defined by:

$$\zeta = \left(\frac{2\psi}{\rho_\infty U_\infty r^2}\right)^{1/2} \tag{5}$$

The thermodynamic state that is determined by the stagnation pressure (Pitot) and the stagnation temperature (adiabatic) is used as a reference state and is denoted by the subscript 0. The Reynolds number Re_0 is based on the viscosity under stagnation conditions,

$$Re_0 = \frac{\rho_\infty U_\infty R_b}{\mu_0} \tag{6}$$

N is the dimensionless viscosity–density product,

$$N = \frac{\mu\rho}{\mu_0\rho_0} \tag{7}$$

and a quantity ϵ has been defined by writing the caloric equation of state in the general form:

$$h = \frac{1}{2\epsilon}\frac{p}{\rho} \tag{8}$$

so that for a perfect gas,

$$\epsilon = \frac{\gamma-1}{2\gamma} \tag{9}$$

Since $p \sim \rho_\infty U_\infty^2$ and $h \sim U_\infty^2/2$ in the shock layer, the density ratio across the shock is of the order of ϵ. Therefore, ϵ has to be much smaller than 1 in order to justify the thin-layer assumption.

In addition to the shock-layer equations, Eqs. (1) and (2), for $\bar{u}$ and $\bar{H}$, boundary conditions are required. At the body surface, given by $\zeta = 0$, ordinary no-slip and no-temperature-jump conditions are used and are applicable to the problem provided that the wall is sufficiently cool in comparison with the stagnation temperature ("highly cooled body") (see Refs. 7 and 8). The no-slip and no-temperature-jump conditions for $\zeta = 0$ can be written as

$$\left.\begin{aligned} \bar{u} &= 0 \\ \bar{H} &= \frac{H_w}{H_\infty} \end{aligned}\right\} \tag{10}$$

($\bar{H} = T_w/T_0$ for a perfect gas) where the subscript w refers to conditions at the body surface (wall). In addition to these inner boundary conditions at the wall, outer boundary conditions at the interface between shock layer and transition zone are needed. The outer boundary conditions could be provided by coupling the shock-layer solution to the transition zone solution at the interface. This somewhat cumbersome procedure can be avoided (at least if nonequilibrium and radiation effects are negligible in the transition zone) by applying the conservation equations in *integral* form to the thin transition layer (see Refs. 6–8). However momentum and energy fluxes due to viscosity and heat conduction have to be taken into account because at low density these effects can be important, even at the outer edge of the shock layer. The following modified Rankine–Hugoniot conditions are obtained, where subscripts 1 and 2, respectively, refer to conditions immediately before and behind the transition zone:

$$\rho_2 v_2 = \rho_1 v_1 \tag{11a}$$

$$p_2 = \rho_1 v_1^2 \tag{11b}$$

$$\rho_1 v_1 (u_2 - u_1) = \left[\mu \frac{\partial u}{\partial y}\right]_2 \tag{11c}$$

$$\rho_1 v_1 (H_2 - H_1) = \left[k \frac{\partial T}{\partial y} + \mu u \frac{\partial u}{\partial y}\right]_2 \tag{11d}$$

where μ is the viscosity, k the thermal conductivity, and u and v are the tangential and normal velocity components, respectively. The modified Rankine–Hugoniot conditions in Eq. (11) change into the ordinary Rankine–Hugoniot conditions when the viscosity and heat conduction terms in Eqs. (11c) and (11d) are omitted. With the modified Rankine–Hugoniot conditions as outer boundary conditions, the flow field of the shock layer can be determined *independently* of the transition zone.

With the introduction of dimensionless dependent variables and the stream function as one of the independent variables into Eqs. (11c) and (11d), and restricting the considerations to the axisymmetric stagnation region, we obtain the outer boundary conditions of the shock layer in the following form for $\zeta = 1$:

$$\left.\begin{aligned} 1 - \bar{u} &= \frac{N}{\epsilon_0 Re_0} \bar{u} \frac{d\bar{u}}{d\zeta} \\ 1 - \bar{H} &= \frac{N}{Pr\, \epsilon_0 Re_0} \bar{u} \frac{d\bar{H}}{d\zeta} \end{aligned}\right\} \tag{12}$$

The pressure, which is approximately constant in the stagnation region of the shock layer, is obtained from Eq. (11b), and is

$$p = \rho_\infty U_\infty^2 \tag{13}$$

It can be seen from Eq. (12) that two flow regimes may be distinguished (with reference to Ref. 7, but defined here without an overlap).

(1) Regime I: $\epsilon_0 Re_0 \gg 1$. Equation (12) yields $\bar{u}(1) = 1$ (i.e., $u_2 = u_1$) and $\bar{H}(1) = 1$ (i.e., $H_2 = H_1$) in agreement with ordinary Rankine–Hugoniot conditions for an adiabatic shock wave. Therefore, regime I includes the ordinary boundary layer regime, the vorticity-interaction regime and the viscous layer regime as defined in Ref. 2.

(2) Regime II: $\epsilon_0 Re_0 = O(1)$. Viscosity and heat conduction immediately behind the transition zone ("shock") give rise to substantial jumps in the tangential velocity components and in the total enthalpy across the shock. Regime II includes (in the terminology of Hayes and Probstein) the incipient merged layer and a major portion of the fully merged layer (see Ref. 8).

The shock-layer equations may be further simplified in regime II (lower Reynolds number regime). In the general case, the right-hand side of the momentum equation, Eq. (1), although of the order of $\epsilon \ll 1$, has to be retained in order to ensure the uniform validity of the solution in the high Reynolds number regime (see Ref. 6). In the low Reynolds number regime, however, the term

$O(\epsilon)$ may be neglected. In addition, if we assume that the viscosity–density product N remains constant across the shock layer, as is often done in boundary layer analysis, then the momentum equation, Eq. (1), is no longer coupled to the energy equation, Eq. (2). Equation (1) has a simple analytical solution given by the linear relationship,

$$\bar{u} = A\,Ch\,\zeta \tag{14}$$

where

$$Ch = \frac{\epsilon_0 Re_0}{N} \tag{15}$$

$$A = \frac{1}{2}\left[\left(1 + \frac{4}{Ch}\right)^{1/2} - 1\right] \tag{16}$$

The important parameter Ch, introduced by Cheng (see Ref. 7) with the symbol K^2, controls the molecular transport effects in the outer part of the shock layer. Since N is of the order of 1, the flow regimes I and II (higher and lower Reynolds number regimes) can be simply defined by $Ch \gg 1$ and $Ch = O(1)$, respectively.

With the introduction of the solution Eq. (14) into the energy equation, Eq. (2), and assuming that the Prandtl number remains constant, the energy equation is reduced to the following linear equation:

$$\frac{d^2\bar{H}}{d\zeta^2} + \frac{Pr}{A}\zeta^2\frac{d\bar{H}}{d\zeta} = 0 \tag{17}$$

III. Modifications Due to Radiation

Radiative shock layers in the higher Reynolds number regime have already been investigated by others (Refs. 10 and 11), but, to the author's knowledge, such investigations do not exist for the lower Reynolds number regime.[2] The following study of radiation effects will therefore be restricted to the lower Reynolds number regime (regime II), where the ordinary Rankine–Hugoniot conditions are not valid, and where radiative transport processes are strongly coupled to viscosity and heat conduction.

[2]After this report was written, the paper "Radiative Transfer in the Low Reynolds Number, Blunt-Body Stagnation Region at Hypersonic Speeds" by J. T. C. Liu and E. Sogame appeared in *AIAA J.*, Vol. 7, No. 7, pp. 1273–1279, July 1969. However, the paper is based on the physically unrealistic assumption of local thermodynamic equilibrium. (Sections IV and V.)

To include radiation in the already rather complex, viscous flow-field analysis seems to be a formidable task; but the low-density regime has its advantages too. The shock-layer thickness is of the order of ϵ_0, and the transition-layer thickness is of the order of Re_0^{-1}. Regime II is characterized by $\epsilon_0 Re_0 \sim 1$, so that shock-layer thickness and transition layer thickness are of the same order of magnitude in this regime. Since the transition layer ("structure" of the shock wave) is several molecular-mean-free-paths thick, the thickness of the shock-layer is also of the order of several mean free paths. On the other hand, the mean free path of radiative absorption is always several orders of magnitude longer than the mean free path of molecular collisions. It follows that only a very small amount of the emitted radiative energy is absorbed within the shock layer because of the low density. In other words, the shock layer may be treated as "optically thin" or "emission dominated." By neglecting absorption of radiation energy the problem is greatly simplified. To include radiation effects in the shock-layer analysis, a term describing the energy losses due to radiative emission must be included. Therefore, the energy equation, Eq. (2), has to be replaced by Eq. (18) (Appendix B):

$$\bar{u}\zeta\frac{d\bar{H}}{d\zeta} + \frac{1}{\epsilon_0 Re_0}\frac{\bar{u}}{\zeta}\frac{d}{d\zeta}\left(\frac{N}{Pr}\frac{\bar{u}}{\zeta}\frac{d\bar{H}}{d\zeta}\right) = \frac{R_b}{U_\infty H_\infty}\frac{E}{\rho} \tag{18}$$

where E is the emitted energy per unit volume and unit time, ρ is the gas density, and the factor $R_b/U_\infty H_\infty$ is a consequence of using the dimensionless variables $\bar{u}$, $\bar{H}$ and ζ. The momentum equation and the solution equation, Eq. (14), for $\bar{u}$ remain unchanged, because radiation pressure certainly can be neglected under atmospheric entry conditions. Substituting the solution Eq. (14) for $\bar{u}$, and again assuming that the Prandtl number remains constant, the energy equation, Eq. (18), is reduced to

$$\frac{d^2\bar{H}}{d\zeta^2} + \frac{Pr}{A}\zeta^2\frac{d\bar{H}}{d\zeta} = \frac{Pr}{A^2 Ch}\frac{R_b}{U_\infty H_\infty}\frac{E}{\rho} \tag{19}$$

Equation (19) differs from the corresponding energy equation for the nonradiative case, Eq. (17), just by the emission term on the right-hand side.

Radiation can also influence the boundary conditions. In the general case (i.e., without additional assumptions), it is not possible to solve the shock-layer equations independently from the transition zone equations, as has been done before in the nonradiative case. The energy

losses due to radiation in the transition zone depend on the temperature distribution in this zone, and (unlike heat conduction effects) they cannot be described in terms of local gradients at the edge of the zone. However, the radiative effects in the transition zone are negligibly small under certain conditions as the following estimate will show. Let the total radiative energy flux toward the body surface be divided into two parts, Q_t and Q_s, such that Q_t is the energy flux due to emission from the transition zone, and Q_s is the energy flux due to emission from the shock layer. The ratio of the two fluxes is of the order of $(E_t\delta_t)/(E_s\delta_s)$, where E_t and E_s are characteristic values of emission E in the transition zone and in the shock layer, respectively, and the terms δ_t and δ_s denote transition zone thickness and shock-layer thickness, respectively. The emitted energy per unit volume and unit time E depends on temperature and density. The temperatures are of the same order of magnitude in both layers. The average density in the transition zone is, however, of the order of the free-stream density (see Ref. 6). Because E is proportional to the density for the type of radiation we are concerned with (see Section V), and since δ_s/R_b is of the order of the density ratio across the "shock," it follows that

$$\frac{Q_t}{Q_s} \sim \frac{E_t\,\delta_t}{E_s\,\delta_s} \sim \frac{\rho_\infty\,\delta_t}{\rho_s\,\delta_s} \sim \frac{\delta_t}{R_b} \tag{20}$$

which is much smaller than 1 according to the basic thin-layer assumption. Equation (20) shows that the dominant amount of radiative flux comes from the shock layer. This result might lead one to conclude that radiation effects in the transition zone are negligible when compared with those in the shock layer, but such a conclusion is not accurate in every case. For instance, if radiation effects are very strong (as they can be at extremely high temperatures and velocities), then the transition zone can be influenced by radiative energy losses to such an extent that the outer boundary conditions for the shock layer are changed considerably. Therefore, it must be assumed that the ratio of radiative energy flux to convective energy flux (the "radiation–convection parameter" Γ) is small when compared with 1 in the transition zone, or, because of Eq. (20), that the radiation–convection parameter is of the order of 1 (or smaller) in the shock layer:

$$\Gamma_s \equiv \frac{E_s\,\delta_s}{\rho_\infty U_\infty H_\infty} = O(1) \tag{21}$$

If this condition holds (and it does hold in the numerical examples given in Section VIII), the radiation effects in the shock-transition zone may be neglected, and the modified Rankine–Hugoniot conditions can be used as outer boundary conditions for the shock layer as in the case without radiation.

IV. Emission Due to Nonequilibrium Radiation

The emitted energy per unit volume and unit time E has to be expressed as a function of the thermodynamic state of a radiating "particle" and, eventually, of the "particle history." Formulating this relationship adequately (to make computation time and accuracy reasonable) was one of the main problems of the present investigation.

Because the regime of interest, given by $Ch = O(1)$, is close to the limits of validity of continuum flow, strong deviations from local thermodynamic equilibrium are to be expected. Nonequilibrium radiation, however, is still rather unexplored, particularly the mechanism by which excited electron states are produced (Refs. 5 and 12–14). Before the model of electron excitation is examined in detail, the assumptions made for other relaxation processes should be briefly reviewed.

Excitation of rotational energy modes does not require many more collisions than excitation of translational degrees of molecular freedom (Ref. 15, pp. 35 and 36). This fact, together with the basic assumption that continuum theory is applicable, justifies assumption I: Translational and rotational energy modes are close to local equilibrium in the whole shock layer, and their small departures from equilibrium can be described by viscosity (including bulk viscosity) and heat conduction.

Excitation of vibrational energy modes, on the other hand, requires many more collisions than excitation of translational and rotational modes; thus, vibrational relaxation times are about an order of magnitude longer than translational and rotational relaxation times. Therefore, vibration will be either frozen or at least far off equilibrium in the shock layer (except for a very thin equilibrium sublayer at the body surface). Because of the lack of data (Ref. 16, pp. 205 and 206) for (1) vibrational relaxation times at the extremely high temperatures that are of interest in the present problem, and (2) relaxation times in various bath-molecules that are present in air or other planetary atmospheres, we shall deal only with the limiting case of frozen vibrational modes. Relaxation times for dissociation and ionization are even much longer than vibrational relaxation times of the same species (see Ref. 15, pp. 35 and 36). These observations lead to assumption II: Vibrational modes, dissociation, and ionization are frozen in the shock layer

(except for a very thin sublayer at the body surface). Hence, provided there is no vibrational excitation, no dissociation, and no ionization in the free stream, it can be assumed that excitation of vibrational energy modes as well as dissociation and ionization are negligible in the shock layer (confirmed by numerical calculation—Ref. 17). Therefore, the state equations of a perfect gas are used in the present calculations. The only nonequilibrium process taken into account is excitation of electron states. Because the sublayer where assumption II is not strictly valid is very thin and cool (for a highly cooled body) when compared with the remaining portion of the shock layer, its influence on radiative heat transfer is certainly small. The convective heat transfer, however, might be influenced by the sublayer to some extent depending on the Lewis number and the catalytic effect of the wall. Although a detailed study of these effects is beyond the scope of the present paper, the results are expected to be similar to those found in ordinary boundary layer theory (see Ref. 3, pp. 180–187) and in Cheng's higher Reynolds number regime (Ref. 17).

In accordance with assumption II and the density and velocity range of interest, the principal contributions to nonequilibrium radiation arise from various molecular band systems. The emitted energy per unit volume and unit time for a given molecular band system is proportional to the population of the excited states. For instance,

$$E^{AB^*} \propto n_{AB^*} = N\,[AB^*] \tag{22}$$

where E^{AB^*} is the emitted energy per unit volume and unit time due to the excited molecular state AB^*, n_{AB^*} is the number of excited molecules AB^* per unit volume, $[AB^*]$ is the number of moles of AB^* per unit volume ("mole concentration" of AB^*), and N is Avogadro's number (6.023×10^{23}/mole). The population of the excited state AB^* may be related to the population of the ground state AB by introducing a Boltzmann distribution of the form

$$\frac{[AB^*]}{[AB]} \propto \exp\left(-\frac{T^{AB^*}}{T_e}\right) \tag{23}$$

where T^{AB^*} represents an activation energy (divided by the gas constant), and T_e is a temperature that characterizes the population of the excited electron state (which must not be confused with the temperature of free electrons in a plasma).

Because frozen flow, in regard to dissociation and ionization, has been assumed, the number of ground state molecules per unit mass remains constant during the flow, provided that the change in ground state population due to excitation is negligible [an assumption which is often made (see Ref. 13), and is valid in all cases of present interest]. Therefore, the number density n_{AB} (molecules per unit volume) is proportional to the gas density ρ. By using Eqs. (22) and (23), the emitted energy per unit volume and unit time may be expressed as

$$E^{AB^*} = C^{AB^*}\rho \exp\left(-\frac{T^{AB^*}}{T_e}\right) \tag{24}$$

where C^{AB^*} is a constant.

If the population of the excited state were in local equilibrium with the translational degrees of freedom, the electron temperature T_e would be equal to the translational temperature T, and Eq. (24) would give the equilibrium radiation due to excited state AB^*. However, this equilibrium value is not always equal to the actual emission in a steady state, because an effect called "collision limiting" might have to be taken into account (this effect will be discussed in Section V).

The following three band systems have been identified as dominant for a terrestrial atmosphere (see Ref. 5): $N_2(1+)$, $N_2(2+)$, and $N_2^+(1-)$. According to the assumption that ionization is negligible, the third band system has to be neglected [but even behind a normal shock wave, where ionization has to be taken into account, the $N_2^+(1-)$ system gives only a small amount of the total radiation (see Ref. 12, Fig. 25)]. For the nitrogen first positive and second positive band systems, and with 78 mole-% N_2 in air, the constants in the following tabulation have the values indicated (see Refs. 5 and 14):

N_2 band system	C, W/g	T, 10^3°K
1+	5.1×10^{10}	85
2+	7.0×10^{12}	129.5

The equilibrium emission from the $N_2(1+)$ and $N_2(2+)$ band systems, respectively, is then given by

$$\left.\begin{aligned} E_e^{1+} &= C^{1+}\rho \exp\left(-\frac{T^{1+}}{T}\right) \\ E_e^{2+} &= C^{2+}\rho \exp\left(-\frac{T^{2+}}{T}\right) \end{aligned}\right\} \tag{25}$$

V. Rate Equations

It takes a certain time for the excited electron states to reach equilibrium or, in case of collision limiting, their steady-state population. This relaxation time strongly effects the total amount of nonequilibrium radiation in the shock layer. It has been assumed, on the basis of earlier experiments and estimates (Refs. 5 and 12), that the electron temperature T_e closely follows the vibrational temperature. Newer measurements (Ref. 14) indicate, however, that the relaxation times for electron excitation are considerably smaller than the vibrational relaxation times, so that the electron temperature T_e seems to be more strongly coupled to the translational temperature T than to the vibrational temperature. This fact justifies our model of frozen vibrational modes and nonequilibrium radiation.

To formulate a rate equation for electron excitation, the reactions involved in the problem are considered. Excitation and de-excitation of molecular species AB and AB^*, respectively, by collisions with a partner M follow the reaction

$$AB + M \underset{D}{\overset{E}{\rightleftarrows}} AB^* + M \tag{26}$$

In addition to this collision reaction, AB^* can also be de-excited by emission of a photon according to the reaction

$$AB^* \rightarrow AB + h\nu \tag{27}$$

where h is the Planck constant, and ν is the frequency. Absorption of photons is neglected because of the low gas density as discussed in Section IV. According to reaction Eqs. (26) and (27), a rate equation can be written in terms of mole concentrations in the following form (see Ref. 5):

$$\frac{d[AB^*]}{dt} = k_E[AB]\,[M] - k_D[AB^*]\,[M] - \frac{1}{\tau_R}[AB^*] \tag{28}$$

where k_E and k_D are the rate constants for excitation and de-excitation by two-body collisions, and τ_R is the radiative lifetime of the excited state AB^*. It should be noted that $1/\tau_R$ specifies the number of radiative transitions per unit time and may be called a radiative transition rate. The ratio k_E/k_D is known as the equilibrium constant, and it determines the equilibrium population. Therefore,

$$\frac{k_E}{k_D} = \frac{[AB^*]_e}{[AB]} \tag{29}$$

with $[AB^*]_e$ denoting the equilibrium concentration of excited molecules AB^* (in a collision-dominated state). By introduction of a collision time τ_c defined in Ref. 5 as

$$\tau_c = \frac{1}{k_D[M]} \tag{30}$$

and replacing k_E by means of Eq. (29), the rate equation, Eq. (28), becomes

$$\frac{d[AB^*]}{dt} = \frac{1}{\tau_c}([AB^*]_e - [AB^*]) - \frac{1}{\tau_R}[AB^*] \tag{31}$$

This rate equation contains concentrations of excited molecules AB^* only. Because the emission due to the excited state AB^* is proportional to the concentration $[AB^*]$ according to Eq. (22), $[AB^*]$ may be replaced by E^{AB^*} in the rate equation, Eq. (31). Collecting the various excited states that contribute to the $N_2(1+)$ and $N_2(2+)$ band systems, and denoting the emissions due to the $N_2(1+)$ and $N_2(2+)$ system by E^{1+} and E^{2+}, respectively, the following "rate equations" for E^{1+} and E^{2+} are obtained:

$$\left.\begin{aligned} \frac{dE^{1+}}{dt} &= \frac{1}{\tau_c^{1+}}(E_e^{1+} - E^{1+}) - \frac{1}{\tau_R^{1+}}E^{1+} \\ \frac{dE^{2+}}{dt} &= \frac{1}{\tau_c^{2+}}(E_e^{2+} - E^{2+}) - \frac{1}{\tau_R^{2+}}E^{2+} \end{aligned}\right\} \tag{32}$$

The quantities τ_c^{1+} and τ_c^{2+} have been introduced as average values of all collision times belonging to the $N_2(1+)$ and $N_2(2+)$ band systems, respectively, and τ_R^{1+} and τ_R^{2+} similarly represent average values of all radiative lifetimes belonging to the $N_2(1+)$ and $N_2(2+)$ systems, respectively. The equilibrium values E_e^{1+} and E_e^{2+} are taken from Eq. (25), and the total energy emitted per unit time and unit volume is given by

$$E = E^{1+} + E^{2+} \tag{33}$$

Some interesting features of the excitation process may be seen from Eq. (32). The emission from a steady state (given by $dE/dt = 0$) is obtained as

$$E_{ss} = \frac{E_e}{1 + \frac{\tau_c}{\tau_R}} \tag{34}$$

where the superscript 1+ or 2+ has been omitted for simplicity. It can be seen from Eq. (34) that the steady-state emission is smaller than the equilibrium value by the factor $[1 + (\tau_c/\tau_R)]^{-1}$. At high densities there are many collisions within a radiative lifetime, the ratio τ_c/τ_R is small, and the steady-state emission is approximately equal to equilibrium emission. At very low densities, however, the number of collisions per unit time can be so small in comparison with the radiative transition rate that the equilibrium population of the excited (radiating) states cannot be maintained against the depopulation due to photon emission. In this case, τ_c/τ_R is of the order of 1 or even larger, and the steady-state emission is substantially smaller or even much smaller than the corresponding equilibrium value. The emission is said to be "collision limited" (see Refs. 5 and 12).

Each of the rate equations, Eq. (32), can be rewritten, with the use of Eq. (34), in the form of an ordinary relaxation equation,

$$\frac{dE}{dt} = \frac{1}{\tau_{\text{eff}}}(E_{\text{ss}} - E) \tag{35}$$

with an effective relaxation time defined by

$$\tau_{\text{eff}} = \frac{\tau_c}{1 + \dfrac{\tau_c}{\tau_R}} \tag{36}$$

Here again the superscripts 1+ and 2+ have been omitted. In the limiting case of very high density, Eq. (36) is reduced to

$$\frac{\tau_c}{\tau_R} \to 0, \qquad \tau_{\text{eff}} = \tau_c \tag{37}$$

and the case of very low density (that is the strongly collision limited case), yields

$$\frac{\tau_c}{\tau_R} \to \infty, \qquad \tau_{\text{eff}} = \tau_R \tag{38}$$

That means the effective relaxation process towards the steady-state emission is controlled by collisions in the high-density case, whereas in the low-density case it is controlled by radiative de-excitations.

To apply the rate equations, Eq. (32), to the flow field of interest, d/dt must be interpreted as a substantial (particle-fixed) derivative and, therefore, replaced by $[u(\partial/\partial x) + v(\partial/\partial y)]$. With the reintroduction of the dimensionless variable ζ discussed in Section II, the rate equations can be written in the following form, and are valid in an axisymmetric stagnation region:

$$\left.\begin{aligned} A\,Ch\,\zeta^2 \frac{dE^{1+}}{d\zeta} + \frac{R_b}{U_\infty \tau_c^{1+}}(E_e^{1+} - E^{1+}) \\ - \frac{R_b}{U_\infty \tau_R^{1+}} E^{1+} = 0 \\ A\,Ch\,\zeta^2 \frac{dE^{2+}}{d\zeta} + \frac{R_b}{U_\infty \tau_c^{2+}}(E_e^{2+} - E^{2+}) \\ - \frac{R_b}{U_\infty \tau_R^{2+}} E^{2+} = 0 \end{aligned}\right\} \tag{39}$$

The initial conditions can be obtained as follows: Since the thickness of the transition zone is of the order of the mean free path for molecular collisions, the assumption is justified that electron excitation immediately behind the transition zone (i.e., at the outer edge of the shock layer) is negligibly small. This assumption is similar to that made by Cheng (see Ref. 8) and confirmed by Chung et al. (Ref. 18) in their investigations of nonequilibrium dissociation in low-density flow. Hence, the following initial condition is used in the present analysis for $\zeta = 1$:

$$E^{1+} = E^{2+} = 0 \tag{40}$$

VI. Collision Time and Radiative Lifetime

The collision time has been defined by Eq. (30) and depends on temperature and density. It contains the rate constant k_D which is a backward rate constant for electron excitation by two-body collisions. Since the activation energy for the backward reaction (de-excitation) is zero, the variation of k_D with temperature T may be expressed (see Ref. 16, p. 225) as

$$k_D = C_D T^{\eta} \tag{41}$$

where C_D and η are constants. Because the flow is treated as frozen with regard to dissociation and ionization, the mole concentrations of all collision partners M are proportional to ρ. Also, because the electron states of both band systems are excited by collisions with the same species (N_2 and O_2 in air), k_D as well as τ_c may be assumed to have the same values for both band systems. It follows from Eq. (30) that

$$\tau_c^{1+} = \tau_c^{2+} = \tau_c = C\left(\frac{\rho_{SL}}{\rho}\right)\left(\frac{T}{10^4}\right)^{\eta} \tag{42}$$

where the reference temperature is 10^4 °K, the reference density ρ_{SL} is the atmospheric density at standard sea-level conditions, and the constant C has the dimension of time. The radiative lifetime, however, is independent of temperature and density according to theoretical investigations (Ref. 19) and is, therefore (for a given band system), a constant.

The four constants C, η, τ_R^{1+}, and τ_R^{2+} cannot be determined by a continuum theory, but they have been calculated from experimental results published previously by other authors; the interested reader may refer to Appendix C. It should be mentioned here, however, that two different experimental results were used. First, the constants C and η were calculated from the time to peak radiation measured behind a normal shock wave in a shock tube (see Ref. 12). Then, with the first result, the radiative lifetimes τ_R^{1+} and τ_R^{2+} were calculated from the results of a collision limiting experiment also described in Ref. 12. The results of the calculations are

$$\left.\begin{aligned} C &= 2.3 \times 10^{-8}\ \text{s} \\ \eta &= -2.26 \\ \tau_R^{1+} &= 1.6 \times 10^{-3}\ \text{s} \\ \tau_R^{2+} &= 5.3 \times 10^{-5}\ \text{s} \end{aligned}\right\} \tag{43}$$

It should be noted that these values are not very accurate, although they are based on the best experimental results available at the present time. However, the radiative emission is influenced considerably by those constants. Therefore, measurements that enable the collision time for electron excitation and radiative lifetime to be determined more accurately would be very useful and desirable.

VII. Method of Solution

The set of differential equations describing the low-density shock-layer flow with nonequilibrium radiation is now complete. It consists of the energy equation, Eq. (19), which contains an energy-emission term, and of the two rate equations, Eq. (39), for the emitted energy due to the two molecular bands of interest. For the equation of state, $\rho = \rho(p,h)$, the perfect-gas relation is used (as justified in Section V) and can be written for the stagnation region by use of Eq. (13) in the form

$$\rho = \frac{2\gamma}{\gamma - 1}\,\frac{\rho_\infty}{H} \tag{44}$$

The rarefaction parameter Ch, defined by Eq. (15), can be written with

$$N = \frac{\mu_s\,\rho_s}{\mu_0\,\rho_0} = \text{constant} \tag{45}$$

as

$$Ch = \frac{\gamma - 1}{2\gamma}\,\frac{\rho_\infty U_\infty R_b}{\mu_s}\,\frac{T_s}{T_0} \tag{46}$$

where the index s refers to a characteristic state ($T = T_s$, $p = \rho_\infty U_\infty^2$) of the shock layer. Replacing N by a constant according to Eq. (45) simplifies the numerical calculations. For a perfect gas under constant pressure (stagnation region), this procedure corresponds to the assumption of a linear viscosity–temperature relationship. Although the linear temperature dependence of the viscosity is rather unrealistic in the case of large temperature variations, good results for heat transfer are obtained if a suitable reference temperature T_s is chosen (Refs. 20 and 21). Because the non-adiabatic effects across the transition zone reduce the mean value of temperature in the shock layer (see the numerical results shown in Section VIII), the following reference temperature has been chosen in accordance with the recommendations made in Ref. 21:

$$T_s = \frac{T_0}{5} = \frac{H_\infty}{5c_p} \tag{47}$$

with the specific heat $c_p = 1000$ m²/s²-°K for air. It should be noted that the linear viscosity–temperature relationship has been used only in the numerical integration across the layer. The reference viscosity $\mu_s = \mu(T_s)$, however, has been calculated by using the very accurate formulas that are based on the Lennard–Jones (6–12) potential of the molecular gas theory (Ref. 22, pp. 528–533 and tables I-A and I-M). The Prandtl number has been calculated from Eucken's relation (see Ref. 16, p. 21), which yields $Pr = 0.737$ for $\gamma = 1.4$.

The no-slip and no-temperature-jump conditions, Eq. (10), are used as boundary conditions at the body surface, and the modified Rankine–Hugoniot conditions, Eq. (12), are used as boundary conditions at the shock interface. Thus, the problem has been reduced to a two-point boundary-value problem that can be solved by standard mathematical methods. In this case an iterative initial-value method has been used with an estimated

initial value of $\bar{H}$ at $\zeta = 1$. There is only one minor difficulty that should be mentioned: The stagnation point ($\zeta = 0$) is a singular point of the rate equations, Eq. (39), and the numerical integration method fails there. This difficulty can be overcome by expanding the unknown solution in a power series for small values of ζ. Since the wall temperature is small in comparison with the stagnation temperature, the emission term in the right-hand side of the energy equation, Eq. (19), can be neglected for very small values of ζ. Hence, the following expansion is obtained for $\zeta \ll 1$:

$$\bar{H} = \bar{H}_w + \left(\frac{d\bar{H}}{d\zeta}\right)_w \zeta + O(\zeta^4) \tag{48}$$

where the index w refers to values at the wall ($\zeta = 0$). Equation (48) shows that for small values of ζ the function $\bar{H}(\zeta)$ may be approximated by a linear relationship of very high accuracy (relative error of order ζ^3). This procedure was used to replace the boundary condition at the singular stagnation point by an equivalent boundary condition at a neighboring point.

After the equations with ζ as independent variable have been solved, the solution may be retransformed into the boundary-layer coordinate system by means of the equation

$$\frac{y}{R_b} = \frac{1}{A\,Ch}\int_0^\zeta \frac{\rho_\infty}{\rho}\,d\zeta \tag{49}$$

which gives the physical distance from the body surface in terms of the body nose radius.

Finally, the heat transfer coefficient, defined as heat flux toward body surface divided by $\rho_\infty U_\infty(H_\infty - H_w)$, may be calculated. The total heat transfer is divided into two parts, one due to convection and the other one due to radiation. The convective part of the heat transfer coefficient at the stagnation point may be obtained from

$$C_H^C \equiv \frac{k\left(\frac{\partial T}{\partial y}\right)_w}{\rho_\infty U_\infty(H_\infty - H_w)} = \frac{A}{Pr\left(1 - \frac{T_w}{T_0}\right)}\left(\frac{d\bar{H}}{d\zeta}\right)_w \tag{50}$$

The heat transfer coefficient due to radiative heat flux toward a black (perfectly absorbing) surface, is given by

$$C_H^R = \frac{1}{2\rho_\infty U_\infty(H_\infty - H_w)}\int_0^{\delta_s} E\,dy$$

$$= \frac{R_b}{2A\,Ch\,U_\infty H_\infty\left(1 - \frac{T_w}{T_0}\right)}\int_0^1 \frac{E}{\rho}\,d\zeta \tag{51}$$

In deriving Eq. (51), the following assumptions have been used:

(1) The contribution of the transition zone to the total radiative flux is negligible.

(2) The shock layer is optically thin.

(3) The shock layer is geometrically thin so that the curvature of the radiating layer may be neglected, which gives rise to a fractional error of the order of $(\delta_s/R_b)^{1/2}$.

For a body surface with a gray (or average) absorptivity a_w, the coefficient of total heat transfer at the stagnation point is finally given by

$$C_H = C_H^C + a_w C_H^R \tag{52}$$

VIII. Results and Conclusions

Numerical calculations have been carried out for the stagnation region of a blunt body traveling in a terrestrial atmosphere. The body surface has been assumed to be sufficiently cool so that T_w/T_0 may be taken as zero. The following parameters have been chosen in the examples shown in Figs. 3–6: Free-stream velocity $U_\infty = 11$ km/s, body radius $R_b = 1$ m, and free-stream density $\rho_\infty = 6.0 \times 10^{-7} \times \rho_{SL}$, which corresponds to an altitude of about 100 km. The shock-layer of Reynolds number (based on the reference temperature T_s) is 40, and Cheng's rarefaction parameter is 1.1, indicating that non-adiabatic effects across the shock transition zone are important. Figure 3 shows the total enthalpy in the shock layer as a function of the dimensionless variable ζ. Because of radiation effects, the total enthalpy in the shock layer is lower than it would be if there were no radiation; however, this result was to be expected. More interesting is the value of the total enthalpy at the outer edge

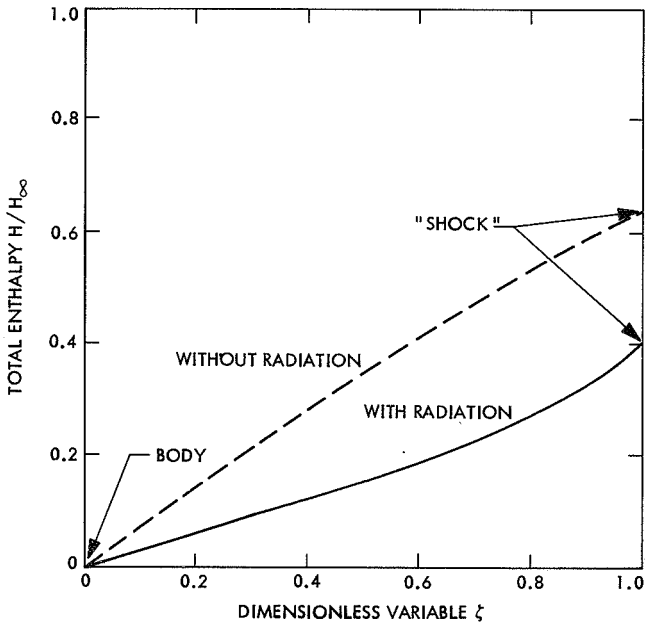

Fig. 3. Total enthalpy as a function of the dimensionless variable ζ

of the shock layer (denoted by the word "shock" in the figures, which stands for "shock interface" or, more specifically, "inner edge of the shock transition zone"). For an adiabatic shock wave, that follows the *ordinary* Rankine–Hugoniot conditions, the total enthalpy remains unchanged, and the initial point of the total enthalpy curve would be $H/H_\infty = 1.0$. However, because of viscosity and heat conduction immediately behind the shock, the total enthalpy at this point is reduced according to the *modified* Rankine–Hugoniot conditions and this effect becomes stronger with decreasing rarefaction parameter Ch. Figure 3 shows that because of radiation the non-adiabatic effect in the shock becomes even stronger. Hence, including radiation has qualitatively the same effect as decreasing the rarefaction parameter Ch or (with ϵ and N fixed) decreasing the Reynolds number Re_0. It should be noted that this effect is *not* due to radiative energy losses in the transition zone (shock), because these energy losses have been neglected in this analysis (see Section IV)! The reason for the additional reduction of total enthalpy immediately behind the shock is to be found in the larger temperature gradient there, which is caused by radiative emission from the shock layer itself. This larger temperature gradient increases the conductive heat flux away from the shock. That is, the radiative emission from the shock layer increases the effect of heat conduction on the shock.

In Fig. 4 the translational temperature is shown as a function of distance from the body surface. The increase of the temperature gradient immediately behind the shock due to radiation effects is clearly seen. Two additional effects may also be noticed: Both the mean temperature in the shock layer and the thickness of the shock layer are reduced by radiation effects.

Figure 5 shows the distribution of the emitted energy per unit volume and unit time over the shock layer. The main contribution comes from the $N_2(2+)$ band, the $N_2(1+)$ system contributes comparably little to the total emission. With E being determined, it is possible to determine if the condition imposed by Eq. (21) holds. Identifying the characteristic shock-layer emission E_s with the maximum emission E_{max} in the shock layer (which yields a very conservative estimate for Γ_s), we obtain $\Gamma_s = 1.0$. Even if the flight speed is increased from 11 to 15 km/s, Γ_s is raised to 1.4 and Eq. (21) is still satisfied.

Profiles of translational temperature and of the electron temperatures correlated with the $N_2(1+)$ and $N_2(2+)$ bands are plotted in Fig. 6. The electron temperatures T_e^{1+} and T_e^{2+} are defined as those temperatures by which T_e in Eq. (25), has to be replaced in order to obtain the actual emissions E^{1+} and E^{2+}, respectively, instead of the equilibrium values (see Eq. 24). The results show that the translational temperature is followed more closely by T_e^{2+} than by T_e^{1+}, although the 2+ band system is affected more strongly by collision limiting than is the 1+ system. The reason is that the effective relaxation

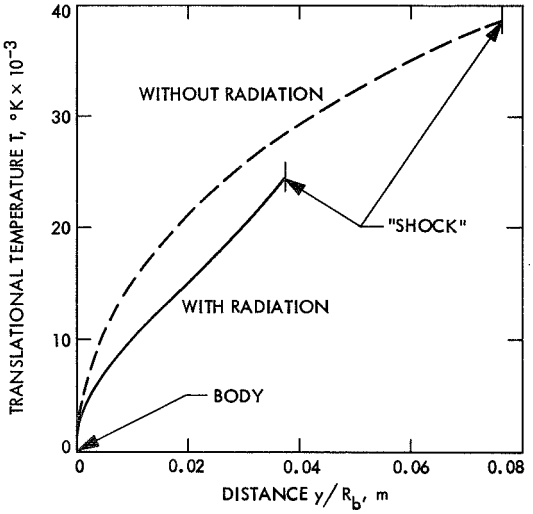

Fig. 4. Profile of translational temperatures in the shock layer

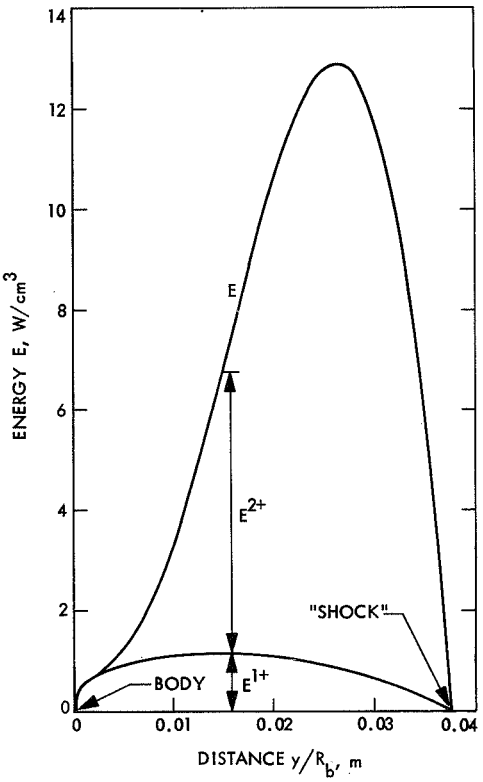

Fig. 5. Radiative emission in the shock layer

time is much shorter for the 2+ band than for the 1+ band (see Eqs. 38 and 43). The remarkably fast increase of the electron temperatures immediately behind the shock indicates that the transition zone, although neglected in the initial conditions of the rate equations, might have some influence on the nonequilibrium process. Also, the electron temperatures near the body are higher than the translational temperature. This indicates some kind of "freezing" in the relaxation process of electron de-excitation.

Values for the heat-transfer coefficient (in air) as a function of free-stream density are presented in Fig. 7. The heat transfer coefficient is divided into convective and radiative expressions, C_H^c and C_H^R, respectively. The total heat-transfer coefficient for a non-black-body surface, therefore, is within the ranges labeled C_H^R in Fig. 7, depending on the wall-absorptivity a_w and given by Eq. (52). Although the velocity is not extremely high, the radiative contribution to the total heat transfer is seen to be quite important. Figure 7 also shows the expected result that the ratio of radiative to convective heat transfer becomes larger with increasing density. For the purpose of comparison, results are given for the case where radiation is omitted in the heat-transfer calculation as well as in the flow-field analysis (energy equation).

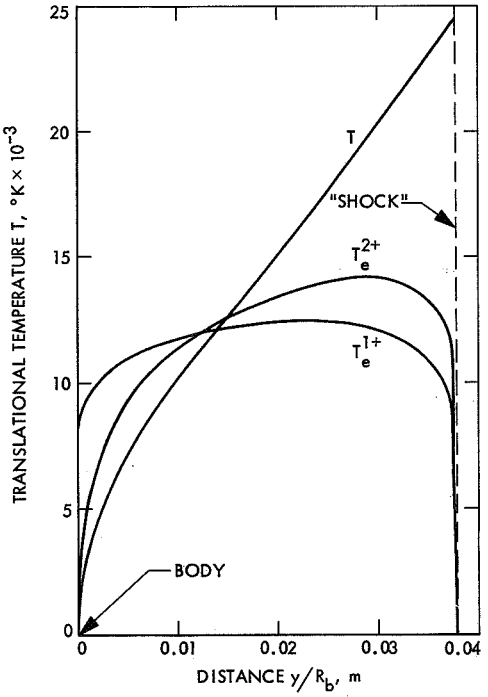

Fig. 6. Profile of translational and electron temperatures

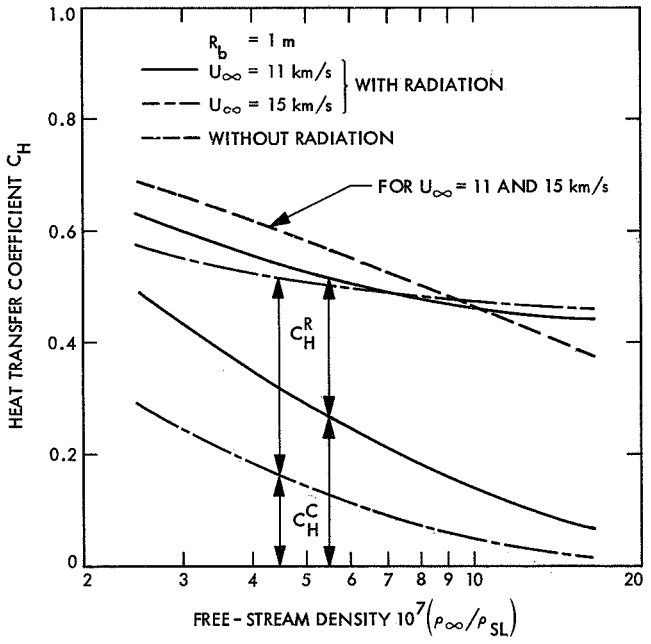

Fig. 7. Convective and radiative contributions to heat transfer in air at an axisymmetric stagnation point

The results presented in Figs. 3–7 show that nonequilibrium radiation influences flow field and heat transfer considerably even at parabolic speeds and low densities (merged layer regime). This is in contradiction with estimates made by Teare, et al., (see Ref. 5) some years ago. However, those estimates are not satisfactory for several reasons. The first, and probably most important, reason is that the radiative heat transfer was *under*estimated by a factor of about 30, because the de-excitation cross section that was used for estimating collision-limiting effects is too high by that factor according to newer measurements (see Ref. 12). The second reason is that the convective heat transfer was *over*estimated because boundary-layer formulas were used, which give overly high convective heat transfer rates in the low-density regime. And finally, the coupling between radiation and convection (including heat conduction) was not taken into account by those estimates, but this effect plays an important role, as the present results show.

The low-density flow without radiation is, of course, governed by the Reynolds number similarity, which permits correlation of flow fields with different body sizes R_b and free-stream densities ρ_∞ by preserving the product $R_b\rho_\infty$. It can be concluded from Eqs. (19), (39), (42), and (43) that this similarity law does not hold when nonequilibrium radiation and its interaction with the flow field are taken into account. Numerical examples are shown in

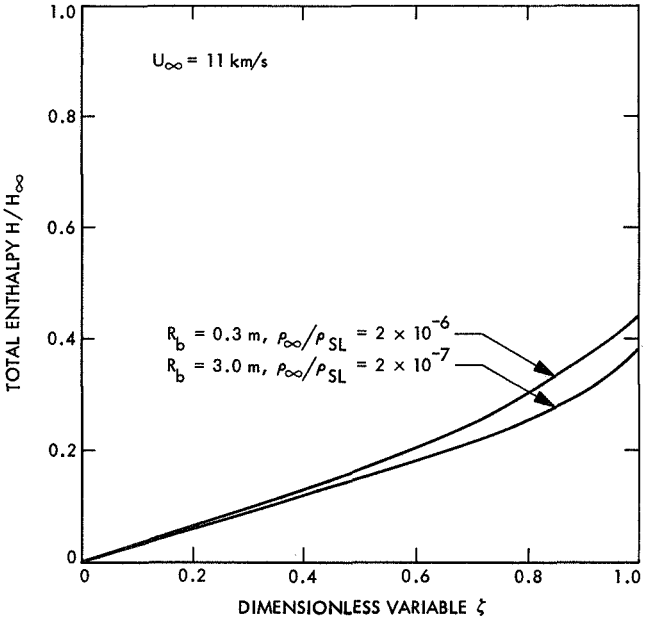

Fig. 8. Total enthalpy solution for different body sizes in air with $R_b\rho_\infty$ held constant

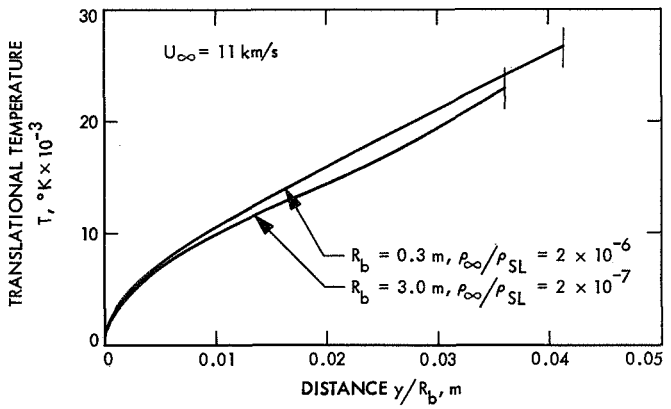

Fig. 9. Profile of translational temperature solution for different body sizes in air with $R_b\rho_\infty$ held constant

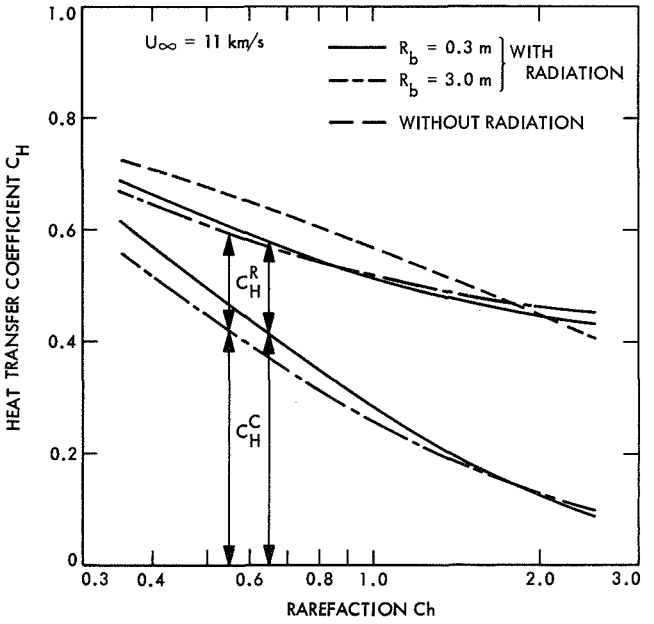

Fig. 10. Convective and radiative heat transfer solutions for different body sizes in air with $R_b\rho_\infty$ held constant

Figs. 8–10. The velocity U_∞ was again chosen to be 11 km/s, and two different body sizes (R_b = 0.3 and 3.0 m) were investigated with the product $R_b\rho_\infty$ held constant. Enthalpy and temperature profiles (Figs. 8 and 9, respectively) are different in the two cases, and so are the heat-transfer coefficients C_H^C and C_H^R as functions of Cheng's rarefaction parameter Ch (Fig. 10), whereas in the nonradiative case the heat transfer coefficient is a function of Ch only (in the present approximation). However, the numerical calculations also show that the results for different body radii with $R_b\rho_\infty$ and U_∞ fixed are but slightly different,

apparently because several different effects partly cancel each other. That is, in rough, approximate calculations, one may correlate radiative flow fields of different body sizes or different free-stream densities by holding both the free-stream velocity and the product $R_b\rho_\infty$ constant.

These results and the assumptions that have been made suggest the following future studies:

(1) Elimination of the assumption expressed in Eq. (21), and solution of the "full" two-layer problem (radiative energy losses taken into account in the transition zone as well as in the shock layer).

(2) Inclusion of finite relaxation times (rate constants) for vibration, dissociation, and ionization into the nonequilibrium process.

Although these generalizations will considerably increase the complexity of the problem, the computation time is expected to be sufficiently short to make some numerical cases feasible, against which the results of the present "reduced" problem can be checked.

Appendix A

Limit of Continuum Theory

The basic condition for continuum flow in the case of a blunt body is the condition

$$\frac{\lambda_s}{\delta_s} \ll 1 \tag{A-1}$$

where λ_s is the collision mean free path behind a normal shock, and δ_s is the thickness of the shock layer (see Ref. 2, pp. 370–380). According to the kinetic theory of gases, the mean free path is of the order of

$$\lambda_s \sim \frac{\mu_s}{\rho_s a_s} \tag{A-2}$$

with μ_s, ρ_s, and a_s as characteristic values of viscosity, density, and speed of sound in the shock layer, respectively. By the application of well known gas dynamical relationships together with the fact that δ_s/R_b is of the order of the density ratio ρ_∞/ρ_s, we obtain for hypersonic flow

$$\frac{\lambda_s}{\delta_s} \sim \frac{\mu_s}{\rho_s a_\infty}\left(\frac{T_\infty}{T_s}\right)^{1/2} \sim \left(\frac{2}{\gamma-1}\right)^{1/2} \frac{\mu_s}{\rho_\infty U_\infty R_b}\frac{R_b}{\delta_s}\frac{\rho_\infty}{\rho_s}$$

$$\sim \frac{\left(\frac{2}{\gamma-1}\right)^{1/2}}{Re_s} \tag{A-3}$$

where Re_s is the shock-layer Reynolds number defined by

$$Re_s = \frac{\rho_\infty U_\infty R_b}{\mu_s} \tag{A-4}$$

Hence the condition for continuum flow, Eq. (A-1), may be written as

$$Re_s^{-1} \ll \left(\frac{\gamma-1}{2}\right)^{1/2} < 1 \tag{A-5}$$

Appendix B

Governing Equations of Shock Layer and Transition Zone Including Radiation Effects

In this investigation of plane or axisymmetric steady flow, a boundary-layer coordinate system x,y is used (see Fig. 2). Let the layer in which the flow quantities are substantially different from the free-stream conditions be optically thin (no self-absorption) and also geometrically thin; i.e.,

$$\left.\begin{aligned} \frac{\partial}{\partial x} &\ll \frac{\partial}{\partial y} \\ Ky &\ll 1 \end{aligned}\right\} \tag{B-1}$$

where K is the longitudinal body curvature, defined as positive if the body is convex. The conservation equations of a viscous, heat-conducting, and radiation-emitting fluid can then be written for continuity, momentum, and energy as shown in Eqs. (B-2–B-4), respectively.

$$\frac{\partial}{\partial x}(r^j \rho u) + \frac{\partial}{\partial y}(r^j \rho v) = 0 \tag{B-2}$$

$$\rho u \frac{\partial u}{\partial x} + \rho v \frac{\partial u}{\partial y} + \frac{\partial p}{\partial x} = \frac{\partial}{\partial y}\left(\mu \frac{\partial u}{\partial y}\right) \tag{B-3a}$$

$$\rho u \frac{\partial v}{\partial x} + \rho v \frac{\partial v}{\partial y} - Ku^2\rho + \frac{\partial p}{\partial y} = + \frac{\partial}{\partial y}\left[\left(\frac{4}{3}\mu + \mu'\right)\frac{\partial v}{\partial y}\right] + \frac{\partial}{\partial y}\left[\left(\mu' - \frac{2}{3}\mu\right)\frac{\partial u}{\partial x}\right] + \mu \frac{\partial^2 u}{\partial x \partial y} \tag{B-3b}$$

$$\rho u \frac{\partial H}{\partial x} + \rho v \frac{\partial H}{\partial y} = \frac{\partial}{\partial y}\left[k \frac{\partial T}{\partial y} + \mu u \frac{\partial u}{\partial y} + \left(\frac{4}{3}\mu + \mu'\right) v \frac{\partial v}{\partial y}\right] - E \tag{B-4}$$

In these equations u and v are the velocity components in the x and y directions, respectively; k is the coefficient of heat conduction; μ and μ' are the coefficients of shear and bulk viscosity, respectively; H is the total enthalpy defined by

$$H = h + \frac{1}{2}(u^2 + v^2) \tag{B-5}$$

Also, E is the emitted energy per unit time and unit volume; r is the distance of the body surface from the axis of symmetry; and j equals 0 for two-dimensional flow and 1 for axisymmetric flow. It should be noted that in the framework of continuum theory, the Eqs. (B-2–B-4) are valid for the transition zone as well as for the shock layer.

The transition zone (shock structure) has been characterized by Cheng (see Refs. 6 and 8) by

$$\left.\begin{aligned} \frac{u}{v} &= O(1) \\ \frac{\rho}{\rho_\infty} &= O(1) \end{aligned}\right\} \tag{B-6}$$

With the use of these orders of magnitude, several terms in Eqs. (B-2–B-4) can be neglected because of the basic assumption in Eq. (B-1). The resulting equations can be integrated once to obtain the following transition zone equations:

$$\rho v = \rho_1 v_1 \tag{B-7a}$$

$$\rho_1 v_1 u - \mu \frac{\partial u}{\partial y} = \rho_1 v_1 u_1 \tag{B-7b}$$

$$p + \rho_1 v_1 v - \left(\frac{4}{3}\mu + \mu'\right)\frac{\partial v}{\partial y} = p_1 + \rho_1 v_1^2 \tag{B-7c}$$

$$\rho_1 v_1 H - \left[k \frac{\partial T}{\partial y} + \mu u \frac{\partial u}{\partial y} + \left(\frac{4}{3}\mu + \mu'\right) v \frac{\partial v}{\partial y}\right] + \int_\infty^y E\, dy = \rho_1 v_1 H_1 \tag{B-7d}$$

where subscript 1 refers to conditions in the free-stream. Velocity v_1 is negative ($u_1 = U_\infty \cos \beta$, $v_1 = -U_\infty \sin \beta$) according to Fig. 2.

The shock layer, and its equations for various coordinate systems are now considered. With the use of an integral form of the mass conservation law, it follows from the basic thin-layer assumption that the density ratio across the shock has to be small, and with the help of Eq. (B-7) the orders of magnitude are estimated as

$$\left.\begin{aligned} \frac{v}{U_\infty \sin\beta} &= O\left(\frac{\rho_\infty}{\rho}\right) \ll 1 \\ p &= O(\rho_\infty U_\infty^2 \sin^2\beta) \\ u &= O(U_\infty \cos\beta) \end{aligned}\right\} \tag{B-8}$$

With the assumption that $1/\sin\beta = O(1)$ (i.e., the body must not be slender) and neglecting terms $O(\rho_\infty/\rho)$ in Eqs. (B-2—B-4) [except the term $\partial p/\partial x$ in Eq. B-3 in order to keep the equations uniformly valid in the region of very high Reynolds numbers (see Ref. 6)] the following shock-layer equations are obtained:

$$\frac{\partial}{\partial x}(r^j \rho u) + \frac{\partial}{\partial y}(r^j \rho v) = 0 \tag{B-9a}$$

$$\rho u \frac{\partial u}{\partial x} + \rho v \frac{\partial u}{\partial y} + \frac{\partial p}{\partial x} = \frac{\partial}{\partial y}\left(\mu \frac{\partial u}{\partial y}\right) \tag{B-9b}$$

$$-Ku^2\rho + \frac{\partial p}{\partial y} = 0 \tag{B-9c}$$

$$\rho u \frac{\partial H}{\partial x} + \rho v \frac{\partial H}{\partial y} = \frac{\partial}{\partial y}\left(k \frac{\partial T}{\partial y} + \mu u \frac{\partial u}{\partial y}\right) - E \tag{B-9d}$$

It has *not* been assumed that $v/u \ll 1$, so that Eqs. (B-9) are valid in the stagnation region also. Equations (B-9) apply to a general fluid.

To satisfy the continuity equation, Eq. (B-9a), the stream function ψ is introduced by

$$\left.\begin{aligned} \frac{\partial \psi}{\partial x} &= -r^j \rho v \\ \frac{\partial \psi}{\partial y} &= +r^j \rho u \end{aligned}\right\} \tag{B-10}$$

With ψ and $\bar{x} = x$ as independent variables (von Mises coordinates), the following equations of momentum and energy are obtained from Eqs. (B-9):

$$u \frac{\partial u}{\partial \bar{x}} = -\frac{1}{\rho}\frac{\partial p}{\partial \bar{x}} + r^{2j} u \frac{\partial}{\partial \psi}\left(\mu \rho u \frac{\partial u}{\partial \psi}\right) \tag{B-11a}$$

$$\frac{\partial p}{\partial \psi} = \frac{K}{r^j} u \tag{B-11b}$$

$$u \frac{\partial H}{\partial \bar{x}} = r^{2j} u \frac{\partial}{\partial \psi}\left[\rho u\left(k \frac{\partial T}{\partial \psi} + \mu u \frac{\partial u}{\partial \psi}\right)\right] - \frac{E}{\rho} \tag{B-11c}$$

Partial derivatives with respect to x are taken with y held constant, but derivatives with respect to $\bar{x}$ are taken with ψ fixed. It is known from boundary-layer theory that $\partial u/\partial \psi \to \infty$ as $\psi \to 0$. This singularity at the body surface is avoided (see Refs. 7, and 8) by the introduction of the independent variable ζ defined by

$$\zeta = \left[\frac{(1+j)\psi}{\rho_\infty U_\infty r^{1+j}}\right]^{1/2} \tag{B-12}$$

Equations (B-11) can easily be rewritten in terms of ζ and dimensionless variables $\bar{u} = u/U_\infty \cos\beta$ and $\bar{H} = H/H_\infty$. By restricting the applicability of the equations to the stagnation region ($\cos\beta \to 0$) the partial differential equations are reduced to ordinary differential equations. Furthermore, the pressure is constant in the stagnation region of a thin shock layer as can be seen from Eq. (B-11c). Hence, the temperature in the energy equation may be replaced by the enthalpy by means of the general thermodynamic relationship (for p = constant)

$$dh = c_p\, dT \tag{B-13}$$

and the Prandtl number $Pr = c_p\mu/k$ can be introduced without restraints upon the fluid properties. Finally the following equations are obtained by using the definitions supplied by Eqs. (6–8):

$$\bar{u}^2 - \frac{1+j}{2}\zeta\bar{u}\frac{d\bar{u}}{d\zeta} = \left(\frac{1+j}{2}\right)^2 \frac{1}{\epsilon_0 Re_0}\frac{\bar{u}}{\zeta}\frac{d}{d\zeta}\left(N\frac{\bar{u}}{\zeta}\frac{d\bar{u}}{d\zeta}\right) + 2\epsilon\bar{H}\left(1 + \frac{2}{1+j}\int_\zeta^1 \bar{u}\zeta\, d\zeta\right) \tag{B-14a}$$

$$-\frac{1+j}{2}\bar{u}\zeta\frac{d\bar{H}}{d\zeta} = \left(\frac{1+j}{2}\right)^2 \frac{1}{\epsilon_0 Re_0}\frac{\bar{u}}{\zeta} \times \frac{d}{d\zeta}\left(\frac{N}{Pr}\frac{\bar{u}}{\zeta}\frac{d\bar{H}}{d\zeta}\right) - \frac{R_b}{U_\infty H_\infty}\frac{E}{\rho} \tag{B-14b}$$

In the axisymmetric case ($j = 1$), Eq. (B-14a) is identical with Eq. (1) in Section III, and Eq. (B-14b) is identical with Eq. (2) in the nonradiative case ($E = 0$) and with Eq. (18) in the radiative case ($E \neq 0$).

Appendix C

Calculation of Constants C, η, τ_R^{1+}, and τ_R^{2+} From Measurements

Experimental results have been presented by Allen et al. (Ref. 12) for $t_p^L p_1$ vs U_∞ in air, where t_p^L is the time to peak radiation (in μs) measured in the laboratory coordinate system, p_1 is the pressure (in atm) in front of the shock wave, and U_∞ is the shock velocity. The value of t_p^L as a function of the temperature T_2 immediately behind the shock is desired. The measurements were made in a regime where the ordinary Rankine–Hugoniot conditions apply. Moreover, vibration, dissociation, ionization, and electronic excitation are frozen immediately behind the shock. Therefore, the perfect gas relationship

$$T_2 = \frac{U_\infty^2}{2c_p} \tag{C-1}$$

may be used to calculate T_2 (Fig. C-1). The straight line, which has been calculated by the least-squares method, is represented by the equation

$$\log_{10}(t_p^L p_1) = -2.79 - 2.26 \times \log_{10}\left(\frac{T_2}{10^4}\right) \tag{C-2}$$

with t_p^L in μs, p_1 in atm, and T_2 in °K.

Since the temperature in front of the shock is approximately equal to the standard temperature at sea level conditions, p_1 can be replaced by ρ_∞/ρ_{SL} (sea level density ρ_{SL}) to give (in μs)

$$t_p^L \frac{\rho_\infty}{\rho_{SL}} = 1.62 \times 10^{-3}\left(\frac{T_2}{10^4}\right)^{-2.26} \tag{C-3}$$

Gases other than air show times to peak radiation that are remarkably close to the results obtained in air (Ref. 23).

The term t_p^L expresses the observed time between the arrival of the shock and the instant of peak radiation in the laboratory-fixed coordinate system. In the rate equations, however, not the laboratory time but the particle time is relevant. Let t_p^P be the time it takes for a particle to move the distance x_p from the shock wave to the point of peak radiation. Hence, the times t_p^L and t_p^P are related to each other by the following equation (with v as velocity of a particle relative to the shock):

$$U_\infty t_p^L = x_p = \int_0^{t_p^P} v\, dt \tag{C-4}$$

The continuity equation of one-dimensional flow can be used to rewrite Eq. (C-4) as

$$t_p^L = \rho_\infty \int_0^{t_p^P} \frac{dt}{\rho} \tag{C-5}$$

and from the mean-value theorem it follows that

$$t_p^L = \frac{\rho_\infty}{\rho_m} t_p^P \tag{C-6}$$

with ρ_m as the mean value, which is the value of the density at a point somewhere within the time interval $0 \le t \le t_p^P$.

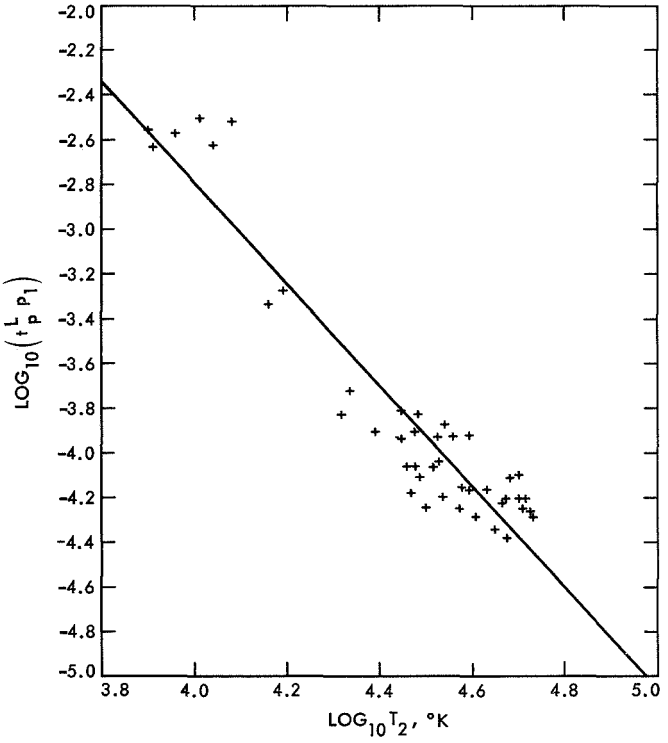

Fig. C-1. Time to peak radiation in air as a function of temperature (after Allen)

A mean collision time $\tau_{c,m}$ can now be defined in accordance with Eq. (42) by

$$\tau_{c,m} = C \frac{\rho_{SL}}{\rho_m} \left(\frac{T_m}{10^4} \right)^{\eta} \tag{C-7}$$

where $T_m = T(\rho_m, p_2)$ is the temperature of the thermodynamic state given by $\rho = \rho_m$ and $p = p_2 = \rho_\infty U_\infty^2$. The collision time controls the time to peak radiation in the particle-fixed coordinate system. Since the measurements that are used to determine the constants C and η have been made in a regime where collision limiting is negligible, the following rate equation and boundary condition apply (see Eqs. 32 and 40):

$$\frac{dE}{dt} = \frac{1}{\tau_c} (E_e - E), \qquad E(0) = 0 \tag{C-8}$$

To obtain an estimate of the relationship between t_p^P and $\tau_{c,m}$, we replace τ_c in Eq. (C-8) by the constant $\tau_{c,m}$, and for the equilibrium emission (which follows the translational temperature) we assume the simple relaxation relation

$$E_e = E^* e^{-t/\tau_i} \tag{C-9}$$

where E^* is a constant, and τ_i is an average (constant) relaxation time of the relaxation processes that control the translational temperature (ionization, dissociation, and internal degrees of freedom). The solution of Eq. (C-8) with E_e replaced by Eq. (C-9) is

$$E = \frac{E^*}{1 - \frac{\tau_{c,m}}{\tau_i}} (e^{-t/\tau_i} - e^{-t/\tau_{c,m}}) \tag{C-10}$$

The time to peak radiation in the particle-fixed coordinate system is obtained from $dE/dt = 0$. Equation (C-10) yields

$$\frac{t_p^P}{\tau_{c,m}} = \frac{\ln \frac{\tau_i}{\tau_{c,m}}}{1 - \frac{\tau_{c,m}}{\tau_i}} \tag{C-11}$$

Experimental results (see Ref. 12, Figs. 14 and 24, and Ref. 14, Fig. 8) show that $\tau_i/\tau_{c,m}$ is of the order of 5–15. By the use of Eq. (C-11), it is found that $t_p^P/\tau_{c,m}$ varies from 2.0 (for $\tau_i/\tau_{c,m} = 5$) to 2.9 (for $\tau_i/\tau_{c,m} = 15$). It is seen that $t_p^P/\tau_{c,m}$ depends but little on $\tau_i/\tau_{c,m}$! Therefore, an average value has been chosen as

$$\frac{t_p^P}{\tau_{c,m}} \approx 2.5 \tag{C-12}$$

The terms t_p^P and $\tau_{c,m}$ in Eq. (C-12) are replaced by means of Eqs. (C-6) and (C-7) to obtain the following equation for the time to peak radiation in the laboratory system:

$$t_p^L = 2.5 \times C \frac{\rho_\infty \rho_{SL}}{\rho_m^2} \left(\frac{T_m}{10^4} \right)^{\eta} \tag{C-13}$$

Comparing this equation with the experimental result, Eq. (C-3), and replacing the density ratio across the (frozen) shock, ρ_∞/ρ_2, by $(\gamma - 1)/(\gamma + 1)$, we obtain

$$\eta = -2.26 \tag{C-14}$$

and

$$C = \frac{1.62 \times 10^{-3}}{2.5} \left(\frac{\gamma + 1}{\gamma - 1} \right)^2 \left(\frac{\rho_m}{\rho_2} \right)^2 \left(\frac{T_2}{T_m} \right)^{\eta} \tag{C-15}$$

The mean values ρ_m and T_m are not known experimentally with any great degree of accuracy. However, because the pressure changes very little in the relaxation zone behind the shock, the power product $(\rho_m/\rho_2)^2(T_2/T_m)^\eta$ is of the order of $(T_2/T_m)^{\eta-2}$. The value of η is very close to 2, and since T_2/T_m is of the order of 2 (see Ref. 14) the power product of the mean values differs very little from 1, and may therefore be dropped in Eq. (C-15). With $\gamma = 1.4$ we finally obtain the result

$$\left.\begin{aligned} C &= 0.023\ \mu s \\ \eta &= -2.26 \end{aligned}\right\} \tag{C-16}$$

After the constants C and η that determine the collision time are obtained, the radiative lifetimes must be evaluated. The results of a collision-limiting experiment that has been performed in pure nitrogen (see Ref. 12) are used for this purpose. The intensity measurements of the $N_2^+(1-)$ band system show that collision limiting is negligible for $U_s = 5.77$ km/s and $p_1 = 100$ μm of Hg, whereas this effect reduces the emitted energy by a factor of approximately 1/2 when $p_1 = 20$ μm of Hg. It follows from Eq. (34) that $\tau_R^{1-} \approx \tau_c$ under the latter conditions, where τ_R^{1-} is the radiative lifetime of the $N_2^+(1-)$ band. Equation (C-17) is obtained with the use of Eqs. (42) and (C-16)

$$\tau_R^{1-} = 4.6 \times 10^{-5}\ \text{s} \tag{C-17}$$

Theoretical investigations (see Ref. 19) show that τ_R is inversely proportional to the transition probability (f-number) and to the square of the frequency. Therefore, the radiative lifetimes of the two band systems of interest in the present analysis, i.e., $N_2(1+)$ and $N_2(2+)$, can be calculated from τ_R^{1-}. On this basis, results have been presented (see Ref. 5) for "critical densities," which are, according to Eq. (42), inversely proportional to the radiative lifetimes. It follows that $\tau_R^{1+}:\tau_R^{2+}:\tau_R^{1-} = 1000:32:28$, and with Eq. (C-17) we finally obtain

$$\left.\begin{aligned} \tau_R^{1+} &= 1.6 \times 10^{-3}\ \text{s} \\ \tau_R^{2+} &= 5.3 \times 10^{-5}\ \text{s} \end{aligned}\right\} \tag{C-18}$$

Nomenclature

A parameter defined in Eq. (16)

$$\left(A = \frac{1}{2}\{[1 + (4/Ch)]^{1/2} - 1\}\right)$$

a_w absorptivity of the wall (body surface)

$[AB]$, $[AB^*]$ mole concentrations of ground-state molecules AB and excited molecules AB^*, respectively

C constant in Eq. (42)

C^{1+}, C^{2+} constants in Eq. (25)

C_H total heat transfer coefficient $[C_H = Q/\rho_\infty U_\infty (H_\infty - H_w)]$

C_H^c, C_H^R heat transfer coefficients due to convection and radiation to a black body, respectively

c_p specific heat at constant pressure

Ch Cheng's rarefaction parameter

$$\left(Ch = \frac{\epsilon_0 Re_0}{N}\right)$$

E radiative energy emitted per unit time and unit volume

H total enthalpy $[H = h + (u^2 + v^2)/2]$

$\bar{H}$ dimensionless total enthalpy $(H = H/H_\infty)$

h specific enthalpy

j for two-dimensional flow $j = 0$; for three-dimensional flow $j = 1$

K longitudinal body curvature

k thermal conductivity

k_E, k_D rate constants for excitation and de-excitation, respectively

M molecule, partner in collision with AB and AB^* species

N dimensionless density–viscosity product $(N = \mu\rho/\mu_0\rho_0)$

p pressure

Pr Prandtl number $(Pr = c_p\mu/k)$

Q total heat flux to surface of body

Q_s, Q_t radiative heat flux due to shock-layer and transition zone emission, respectively

R_b nose radius of body

r distance from the axis of symmetry to a point on the surface of the body

Re_0 Reynolds number at stagnation conditions $(Re_0 = \rho_\infty U_\infty R_b/\mu_0)$

Re_s Reynolds number at shock layer conditions $(Re_s = P_\infty U_\infty R_b/\mu_s)$

T translational temperature

T^{1+}, T^{2+} activation energy constants in Eq. (25)

T_e^{1+}, T_e^{2+} temperatures that characterize the population of the excited electron states in the N_2^{1+} and N_2^{2+} band systems, respectively

t time

t_p^L, t_p^P time to peak radiation in the laboratory-fixed and particle-fixed coordinate systems, respectively

U_∞ free-stream velocity; also the velocity in front of a moving shock wave

u velocity component in the x-direction

$\bar{u}$ dimensionless velocity in the x-direction $(\bar{u} = u/U_\infty \cos\beta)$

v velocity component in the y-direction

x,y boundary-layer coordinate system

β body inclination angle

γ ratio of specific heats

δ_s, δ_t thickness of the shock layer and the transition zone, respectively

ϵ thermodynamic quantity defined by Eq. (8)

ζ dimensionless variable defined by Eq. (5 or B-12)

η constant in Eq. (42)

μ, μ' coefficients of shear and bulk viscosity, respectively

ρ density

ρ_{SL} standard atmospheric density at sea level

$\tau_c, \tau_{eff}, \tau_R$ collision time, effective relaxation time, and radiative lifetime, respectively

ψ stream function

Nomenclature (contd)

Subscripts

e	value at equilibrium conditions
m	mean value in the relaxation zone behind a shock wave
s	characteristic value in the shock layer
ss	value at steady-state conditions
t	characteristic value in the transition zone
w	conditions at the wall (body surface)
0	stagnation conditions
1	conditions in front of the transition zone
2	conditions immediately behind the transition zone or shock wave
∞	conditions in the free stream

Superscripts

$1+, 2+$	first positive and second positive N_2 band systems

Special symbols

$O( )$	of the order of ( )
$\sim$	of the same order of magnitude as
$\approx$	approximately equal to
$\propto$	proportional to

References

1. Probstein, R. F., "Shock Wave and Flow Field Development in Hypersonic Re-Entry," *ARS J.*, Vol. 31, pp. 185–194, 1961.
2. Hayes, W. D., and Probstein, R. F., *Hypersonic Flow Theory*, Chap. X, Academic Press, New York, 1959.
3. Cox, R. N., and Crabtree, L. F., *Elements of Hypersonic Aerodynamics*, Chap. 9. The English Universities Press, London, 1965.
4. Van Dyke, M. D., "Second-Order Compressible Boundary Layer Theory With Application to Blunt Bodies in Hypersonic Flow," in *Hypersonic Flow Research*, pp. 37–76. Edited by F. R. Riddell. Academic Press, New York, 1962.
5. Teare, J. D., Georgiev, S., and Allen, R. A., "Radiation From the Nonequilibrium Shock Front," in *Hypersonic Flow Research*, pp. 281–317. Edited by F. R. Riddell. Academic Press, New York, 1962.
6. Cheng, H. K., "Viscous Hypersonic Blunt-Body Problems and the Newtonian Theory," in *Fundamental Phenomena in Hypersonic Flow*, pp. 90–132. Edited by J. G. Hall. Cornell University Press, Ithaca, N.Y., 1966.
7. Cheng, H. K., "Hypersonic Shock-Layer Theory of the Stagnation Region at Low Reynolds Number," in *Proceedings of the 1961 Heat Transfer and Fluid Mechanics Institute*, pp. 161–175. Edited by R. C. Binder, et al. Stanford University Press, Stanford, Calif., 1961.
8. Cheng, H. K., *The Blunt-Body Problem in Hypersonic Flow at Low Reynolds Number*, Report AF-1285-A-10. Cornell Aeronautical Laboratory, Buffalo, N.Y., 1963.
9. Bush, W. B., "On the Viscous Hypersonic Blunt Body Problem," *J. Fluid Mech.*, Vol. 20, Part 3, pp. 353–367, 1964.

References (contd)

10. Goulard, R., et al., "Radiating Flows During Entry Into Planetary Atmospheres," Paper RE 70, presented at the 19th Congress of the International Astronautical Federation, New York, 1968.

11. Anderson, J. D., Jr., "An Engineering Survey of Radiating Shock Layers," Paper 68-1151, presented at the AIAA Entry Vehicle Systems and Technology Meeting, Williamsburg, Va., 1968.

12. Allen, R. A., Rose, P. H., and Camm, J. C., "Nonequilibrium and Equilibrium Radiation at Super-Satellite Re-Entry Velocities," Paper 63-77, presented at the 31st Annual Meeting of the Institute of the Aerospace Sciences, New York, 1963.

13. Hansen, C. F., and Chapin, C. E., *Nonequilibrium Radiation From the Stagnation Region of High-Velocity Bodies,* Report TR64-02G. Defense Research Laboratories, General Motors Corporation, Warren, Mich., 1964.

14. Allen, R. A., "Nonequilibrium Shock Front Rotational, Vibrational and Electronic Temperature Measurements," *J. Quant. Spectrosc. Radiat. Transfer,* Vol. 5, No. 3, pp. 511–523, 1965.

15. Stupochenko, YE. V., Losev, S. A., and Osipov, A. I., *Relaxation in Shock Waves.* Translation edited by R. E. Lee. Springer-Verlag New York Inc., New York, 1967.

16. Vincenti, W. G., and Kruger, C. H., *Introduction to Physical Gas Dynamics.* John Wiley & Sons, Inc., New York, 1965.

17. Inger, G. R., "Nonequilibrium Hypersonic Stagnation Flow With Arbitrary Surface Catalycity Including Low Reynolds Number Effects," *Int. J. Heat Mass Transfer,* Vol. 9, No. 8, pp. 755–772, Aug. 1966.

18. Chung, P. M., Holt, J. F., and Liu, S. W., "Merged Stagnation Shock Layer of Nonequilibrium Dissociating Gas," *AIAA J.,* Vol. 6, No. 12, pp. 2372–2379, Dec. 1968.

19. Hansen, C. F., "A Radiation Model for Nonequilibrium Molecular Gases," *AIAA J.,* Vol. 2, No. 4, pp. 611–616, Apr. 1964.

20. Eckert, E. R. G., "Engineering Relations for Friction and Heat Transfer to Surfaces in High Velocity Flow," *J. Aeronaut. Sci.,* Vol. 22, pp. 585–587, 1955.

21. Cheng, H. K., and Chang, A. L., "Stagnation Region in Rarefied, High Mach Number Flow," *AIAA J.,* Vol. 1, No. 1, pp. 231–233, Jan. 1963.

22. Hirschfelder, J. O., Curtis, C. F., and Byrd, R. B., *Molecular Theory of Gases and Liquids.* John Wiley & Sons, Inc., New York, 1954.

23. Thomas, G. M., and Menard, W. A., "Experimental Measurements of Nonequilibrium and Equilibrium Radiation From Planetary Atmospheres," *AIAA J.,* Vol. 4, No. 2, pp. 227–237, Feb. 1966. Also available as Technical Report 32-902, Jet Propulsion Laboratory, Pasadena, Calif., 1966.

NASA — JPL — Coml., L.A., Calif.